manner, the overall results for
y and unambiguously extended
/ shapes.

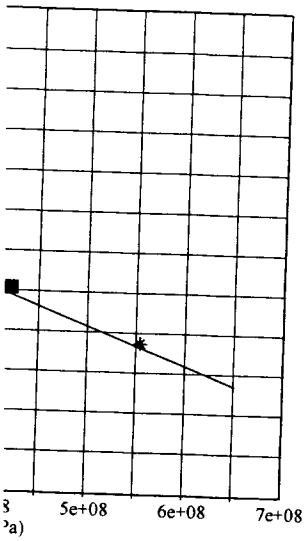

g path in the (p,τ) diagram.

xt of mechanical design, K. Dang
.ectures no 392, Springer-Verlag,

the evaluation of long life fatigue
:. *Conference on life assessment of*
isbon, Portugal, 17–21 Sept. 1984,

s using the theory of critical dis-

oulos, *Fatigue Fract. Eng. Mater.*

'atigue Fract. Eng. Mater. Struct.,

notch; the use of notch stress

MEASUREMENTS FOR MECHANICAL RELIABILITY OF THIN FILMS*

DAVID T. READ
Materials Reliability Division, National Institute of Standards and Technology, Boulder, Colorado

ALEX A. VOLINSKY
Department of Mechanical Engineering, University of South Florida, Tampa, Florida

Abstract This paper reviews techniques for measurement of basic mechanical properties of thin films. Emphasis is placed on the adaptations needed to prepare, handle, and characterize thin films, and on adaptations of fracture mechanics for adhesion strength. The paper also describes a recent development, the use of electrical current as a controlled means of applying thermomechanical stresses to electrical conductors to characterize their fatigue behavior.

Keywords: Delamination, grain size, strain, strength, substrate, testing, tensile, yield strength, Young's modulus

1. Introduction

From the time of Galileo to the late twentieth century, mechanical testing evolved at the macro scale, with specimen dimensions of the order of centimeters and even meters in some cases. This was a natural match to the structures being analyzed, which included bridges, pipelines, pressure vessels, aircraft and their engines, rockets, and so on. The appreciation that larger structures produce mechanical constraints that promote brittle fracture became widespread only after many tragic failures, which are well documented. Wide plate testing was developed to examine the conditions under which a small crack or inhomogeneity such as a weld can be tolerated by a large

* Contribution of the U.S. National Institute of Standards and Technology. Not subject to copyright in the U.S.

G. Pluvinage and A. Sedmak (eds.), *Security and Reliability of Damaged Structures and Defective Materials*,

structural element. The need to control catastrophic brittle failure led to the first serious attempt to understand size effects in mechanical behavior, specifically, the development of structural fracture mechanics in the mid-twentieth century. This understanding was applied both to the structures themselves and to the test protocols, so that specimens small compared to the structures of interest could be used to explore and verify material behavior. These specimens were and still are macroscale: they can be manufactured with lathes and milling machines; they can be mounted by hand with no risk of damage to the specimen; and they can be tested without the need for microscopy.

The next push toward smaller scale mechanical testing came with the rise of thin film technology for microelectronics, and the related micro-electro-mechanical systems (MEMS) technology, where photolithography is used to create structures that provide mechanical functionality with critical dimensions on the scale of micrometers. Analytical tools from the macro world were adapted to design against the surprisingly high stresses that arise in integrated circuits; the source of these stresses is the difference in thermal expansion rate among the different materials that are bonded together in thin layers to produce integrated circuits, combined with the severe temperature excursions seen in these structures in both production and use. But numerical analysis alone was not enough; the results of a numerical analysis depend on the material properties data used, and thin film materials have properties much different from those of the same materials in bulk form. These property differences are a natural consequence of the much different microstructures between thin film and bulk materials. The microstructures are a consequence of the novel production methods used for the thin film materials, for example, physical vapor deposition for thin films as opposed to rolling and annealing for bulk materials. While measurements of basic mechanical properties, such as elastic modulus and yield and ultimate strength, of materials with dimensions around 1 μm are well established and widely practiced, fracture mechanics has recently found a mode of application in the microscale that differs in emphasis from the practice in macroscale structures.

Delamination of thin films from rigid substrates, of which delamination of an aluminum film from a silicon wafer would be a simplified example, is a critical issue for integrated circuits and other thin film structures. This failure mode is of relatively low importance in macroscale structures, which rarely utilize bonds between large flat sheets as critical structural elements. The testing of the adhesion between film and substrate has been attempted by a multitude of approaches, but it is now recognized that the strength of an interface can most accurately and usefully be described in terms from fracture mechanics, in particular, energy per unit area of the bond between

film and substrate and magnitude
Inspection for delaminations, for
applied to larger scale features of i
couched more in terms of the quali
such "quality" criteria are remin
macroscale structures. Finer-scale
down to the use of atomic forc
application to the understanding
100% inspection of every interfa
complex as modern integrated
complex, too numerous, and too cl

This paper reviews technique
properties of thin films, includin
adhesion strength. For films with
these measurements are well dev
understood, and their behavior ca
grain size and dislocation-mediat
macroscale materials. Progress in
nanoscale thicknesses will be not
development, the use of electrical
thermomechanical stresses to elect

2. Mechanical properties meas

This section draws heavily on th
electronics and Photonics: Phy
Reliability," by D. T. Read and A.
use for mechanical characterizatio
and instrumented indentation, also
methods in wide use include wafe
a variety of tests of the adhesion o

2.1. MICROTENSILE TESTING

Tensile testing is the standard m
perties of structural metals. Beca
the gage section, the Young's mo
strength can be obtained from an
was natural to apply this time-test
pull thin films in conventional tes
their substrate. This operation dep
the specimen film, such as water so

film and substrate and magnitude of stress singularities at critical locations. Inspection for delaminations, for example by ultrasonic means, has been applied to larger scale features of integrated circuits. Acceptance criteria are couched more in terms of the quality of the bond than in critical crack sizes; such "quality" criteria are reminiscent of earlier practices in welding in macroscale structures. Finer-scale inspection and quality control techniques, down to the use of atomic force microscopy, are being developed for application to the understanding and detection of delamination. However, 100% inspection of every interface will never be applied to structures as complex as modern integrated circuits; the structures are simply too complex, too numerous, and too cheap, to allow such an effort.

This paper reviews techniques for measurement of basic mechanical properties of thin films, including adaptations of fracture mechanics for adhesion strength. For films with thicknesses on the order of micrometers, these measurements are well developed. The materials are generally well understood, and their behavior can be interpreted using concepts such as grain size and dislocation-mediated plastic strain, which are familiar from macroscale materials. Progress in extending these methods to films with nanoscale thicknesses will be noted. The paper will also describe a recent development, the use of electrical current as a controlled means of applying thermomechanical stresses to electrical conductors.

2. Mechanical properties measurements at the micrometer scale

This section draws heavily on the book chapter "*Thin Films for Microelectronics and Photonics: Physics, Mechanics, Characterization, and Reliability*," by D. T. Read and A. A. Volinsky.[1] The main methods in current use for mechanical characterization of thin films include microtensile testing and instrumented indentation, also referred to as nanoindentation (NI). Other methods in wide use include wafer curvature, the pressurized bulge test, and a variety of tests of the adhesion of a film to its substrate.

2.1. MICROTENSILE TESTING

Tensile testing is the standard means of obtaining basic mechanical properties of structural metals. Because the stress field is uniform throughout the gage section, the Young's modulus, yield strength, and ultimate tensile strength can be obtained from an accurate force-displacement record. So it was natural to apply this time-tested method to thin films. Early attempts to pull thin films in conventional testing machines used specimens lifted from their substrate. This operation depended on special separation layers beneath the specimen film, such as water soluble sodium chloride. Excessive wrinkling

often occurred during placement of the specimen on the grips. Despite the obstacles, meaningful data were gradually obtained. Early tests of metal films revealed the main phenomena still seen today: high strength, and low elongation to failure.[2] There is at present no standard test method for microtensile testing of thin films; individual investigators adapt the standard methods for bulk metal specimens to fit their specific specimen geometry. Standardization is hindered by the multitude of specimen sizes and designs that are in use, which has resulted from the difficulty of fabricating microtensile specimens.

The problems with the early methods led to improved procedures. It became evident that since films in actual devices are always produced on substrates, the use of the substrate to support the thin film specimen is appropriate. But the substrate is always much more massive than the film, so it must be removed at least from beneath the gage section of the specimen. Ding et al.[3] reported the use of a silicon frame design for testing doped silicon. The first realization of this scheme for metal films was the silicon frame tensile specimen.[4] Bulk micromachining of MEMS devices had been developed by this time, demonstrating the concept of etching away a selected portion of the substrate to form a useful device. To produce the silicon frame tensile specimen, photolithographic patterning was used to form a straight and relatively narrow gage section with larger grip sections on a silicon frame. The substrate beneath the gage section was removed by a suitable etchant. The silicon frame, carrying its tensile specimen of a thin film, was mounted on a purpose-built test device capable of supplying force and displacement.[4] The silicon frame was cut, while leaving the specimen undamaged. This step has been accomplished manually with a dental drill, using a temporary clamp to hold the specimen in place, and by the use of a cutting wheel mounted on a moveable stage.[5]

All the tensile testing techniques include measurements of force and displacement. The force is measured using a load cell, either commercial or custom-built. For specimens of thin films with cross sectional areas of the order of 200 μm^2, the force might amount to 0.1 N. Commercial load cells with this range are available. Displacement has been measured by interferometric techniques such as electron speckle pattern interferometry (ESPI), for example as in,[6] or by diffraction from markers placed on the specimen surface.[7] Even with measurement of displacement directly on the specimen gauge section, modulus measurements are difficult. Successful attempts to use grip or crosshead displacement for accurate strain measurements are unknown to this author.

The specimen fabrication challenge with these techniques was the chemical selectivity required to etch through hundreds of micrometers of silicon without damaging the metal specimen. Aqueous hydrazine has been

used, but this material is hazard
of the gage section, 100 μm or
used in interconnect and also with

A new generation of smalle
techniques, has been develope
around 10 μm and the gage len
remains near 1 μm, Figure 1.[8] T
the substrate is removed to a dep
by use of xenon difluoride. Thi
and is very selective for silicon
Young's modulus can usually
Poisson's ratio has been measur
large specimens,[5,9] because the
few-micrometer wide specimen
specimen was loaded by engagin
to a hole in the loading tab, F
micromachining approach is the
a series of face-centered-cubic (F

A new advance is the co-fa
frame that includes a force senso
use inside a transmission electron

A recent round robin show
laboratories in the strength of
most labs required their own u
geometries were produced on the
obtained for polySi were impres
polycrystalline Young's modulu
theoretical strength of a solid.

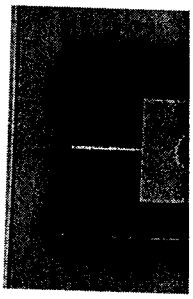

Figure 1. Microtensile specimen of alumi
loading tab, with its 50 μm diameter hole
use in digital image correlation for displa
substrate has been etched away to a depth
lines connecting the field to the loading
testing.

used, but this material is hazardous. Another disadvantage is the large width of the gage section, 100 μm or more, by comparison with the line widths used in interconnect and also with typical film thicknesses of the order of 1 μm.

A new generation of smaller-scale specimens, and complementary test techniques, has been developed. In this version, the specimen width is around 10 μm and the gage length is around 200 μm, while the thickness remains near 1 μm, Figure 1.[8] The surface micromachining concept is used; the substrate is removed to a depth of around 100 μm beneath the specimen by use of xenon difluoride. This etchant is less hazardous than hydrazine, and is very selective for silicon masked by SiO_2, aluminum, copper, etc. Young's modulus can usually be measured in these specimens, but Poisson's ratio has been measured only by special techniques on relatively large specimens,[5,9] because the transverse displacements are so small on a few-micrometer wide specimens. In an early version of this test, the specimen was loaded by engaging a tungsten probe tip, 50 μm in diameter, to a hole in the loading tab, Figure 2. A recent variant of the surface micromachining approach is the membrane deflection tensile test, applied to a series of face-centered-cubic (FCC) metals by Espinosa et al.,[10] Figure 3.

A new advance is the co-fabrication of a specimen and a protective frame that includes a force sensor, Figure 4.[11] This specimen is suitable for use inside a transmission electron microscope (TEM).

A recent round robin showed reasonable agreement among several laboratories in the strength of polySi (polycrystalline silicon), although most labs required their own unique specimen geometry. The different geometries were produced on the same MEMS chip.[12] The strength values obtained for polySi were impressively high, of the order of 1/30 of the polycrystalline Young's modulus, which is the usual estimate of the theoretical strength of a solid.

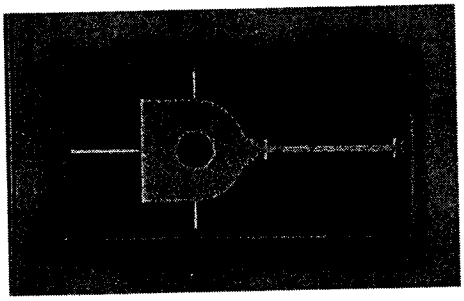

Figure 1. Microtensile specimen of aluminum, fabricated through the MOSIS process. The loading tab, with its 50 μm diameter hole, is to the left. The gauge section, with "ears" for use in digital image correlation for displacement measurement, is to the right. The silicon substrate has been etched away to a depth of 60 μm or more. The three slender aluminum lines connecting the field to the loading tab are tethers that are manually cut just before testing.

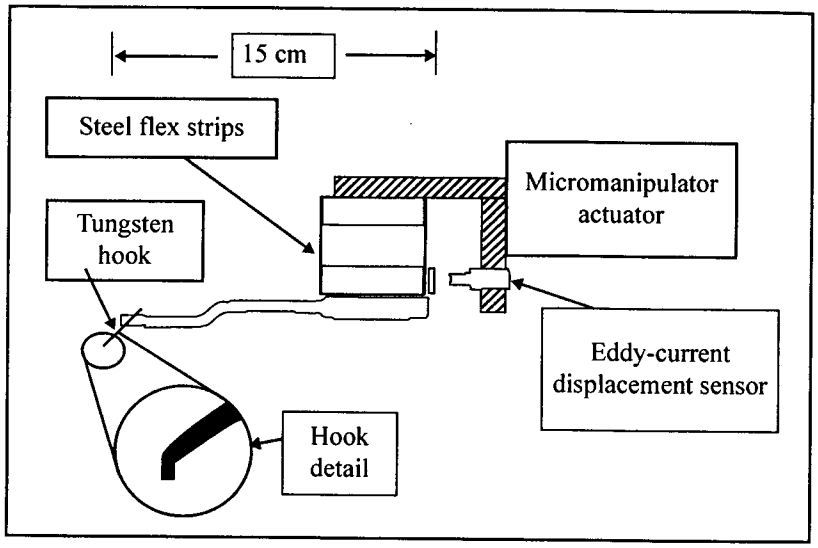

Figure 2. Tungsten "hook" carried by instrumented micromanipulator to load tensile specimen and measure the force.

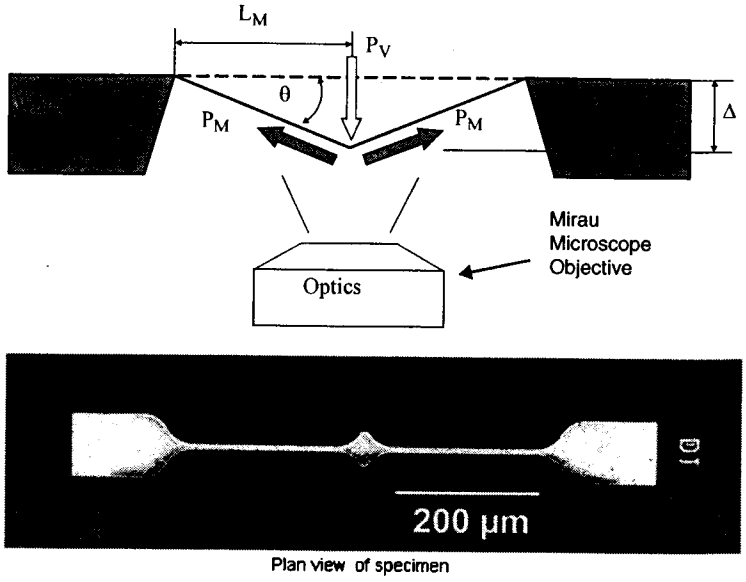

Figure 3. Setup for the membrane deflection tensile test.[10] (Figure courtesy of H. Espinosa).

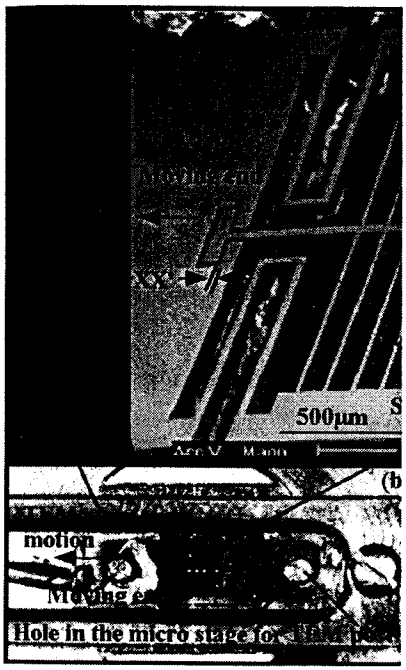

Figure 4. Tensile specimen assembly i
support assembly and force gage for use i

2.2. INSTRUMENTED INDENTAT

The nanoindentation test is simila
performed on a much smaller sca
indenter.[13] The force required to p
material is continuously recorded
indicated schematically in Figure
either on electromagnetic or electrc
resolution is on the order of angsti
very thin (~100 nm) films. The r
similar to one shown in Figure 6, p
material's response to contact de
are the two parameters that can be
load-displacement curve. Elastic p
were originally proposed by Lc
suggested that a linear fit to the u
indentation curve could be used t
from which the reduced elastic mc

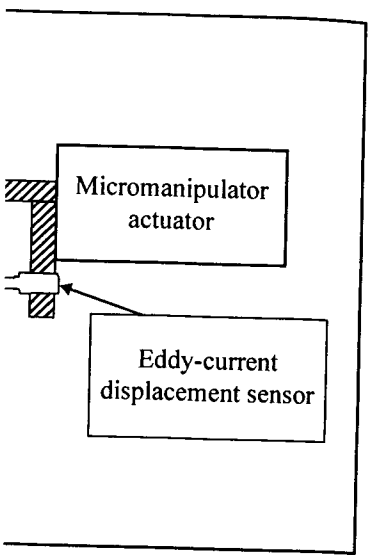

micromanipulator to load tensile specimen

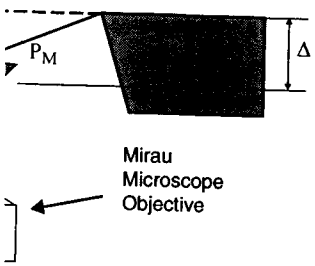

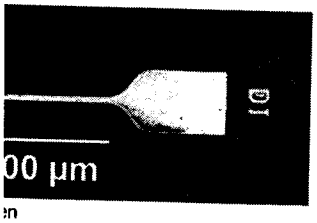

test.[10] (Figure courtesy of H. Espinosa).

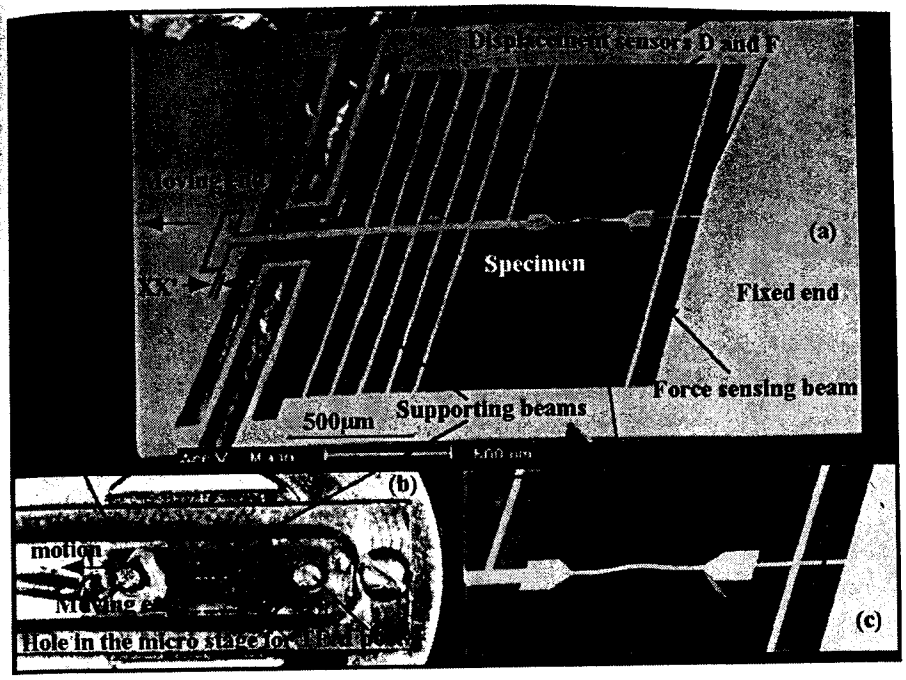

Figure 4. Tensile specimen assembly including aluminum tensile specimen and MEMS support assembly and force gage for use in the TEM.[11] (Figure courtesy of T. Saif.)

2.2. INSTRUMENTED INDENTATION

The nanoindentation test is similar to the conventional hardness test, but is performed on a much smaller scale using specialized equipment – a nano-indenter.[13] The force required to press a sharp diamond indenter into tested material is continuously recorded as a function of the indentation depth, as indicated schematically in Figure 5. The actuation mechanism can be based either on electromagnetic or electrostatic application of force. Since the depth resolution is on the order of angstroms, it is possible to usefully indent even very thin (~100 nm) films. The nanoindentation load–displacement curve, similar to one shown in Figure 6, provides a "mechanical fingerprint" of the material's response to contact deformation. Elastic modulus and hardness are the two parameters that can be readily extracted from the nanoindentation load-displacement curve. Elastic property measurements by nanoindentation were originally proposed by Loubet et al.[14] Later, Doerner and Nix[15] suggested that a linear fit to the upper 1/3 of the unloading portion of the indentation curve could be used to determine film stiffness, $S = dP/dh$, from which the reduced elastic modulus, E_r, could be found as

$$E_r = S\frac{\sqrt{\pi}}{2\sqrt{A}} \tag{1}$$

Here A is the contact area and the reduced modulus is a combined elastic property of the film and indenter material. Since the indenter material itself has finite elastic constants, its deformation contributes to the measured displacement. The reduced modulus E_r is

$$\frac{1}{E_r} = \frac{1-\nu_i^2}{E_i} + \frac{1-\nu_f^2}{E_f} \tag{2}$$

In this equation E is the elastic modulus, ν is the Poisson's ratio, and the subscripts f and i refer to the film and the indenter materials respectively. A more elaborate power law fit to the unloading portion of the load-displacement curve was suggested by Oliver and Pharr,[16] and is widely known as the Oliver and Pharr method.

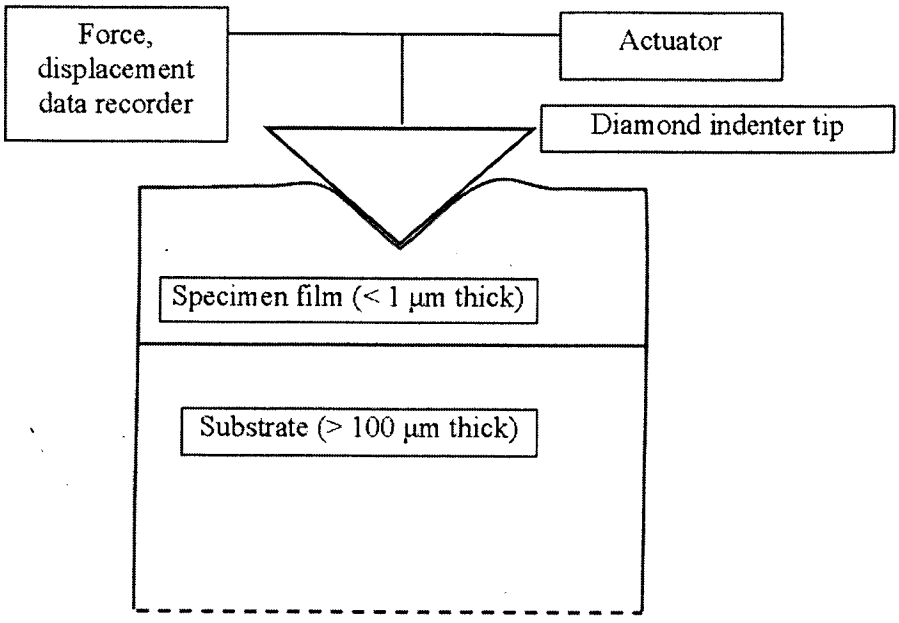

Figure 5. Schematic of instrumented instrumentation measurement.

Hardness H, a material's resistance to plastic deformation, is defined as

$$H = \frac{P_{max}}{A} \tag{3}$$

where A is the projected area of contact (a function of the indentation depth) at the maximum load P_{max}.

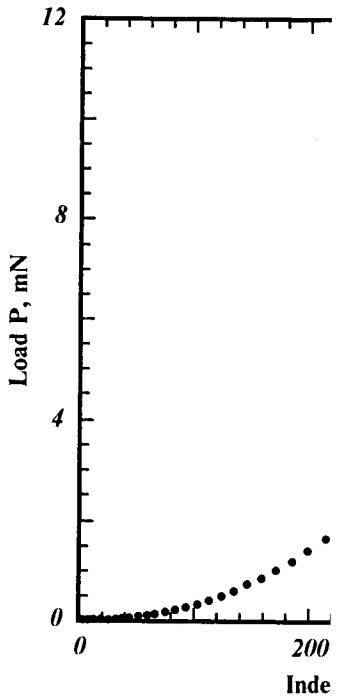

Figure 6. Load–displacement r

The expressions for both e
contact area, which is correlated
through the known geometry of th
a material with known elastic m
sists of indenting a standard mate
to various maximum indentation
from tip calibration, various tij
common being the Berkovich
manufacturing standpoint, a thr
and the tip radius can be as sha
used, and include Vickers (a st
conical and wedge indenters. Th
tip geometry as

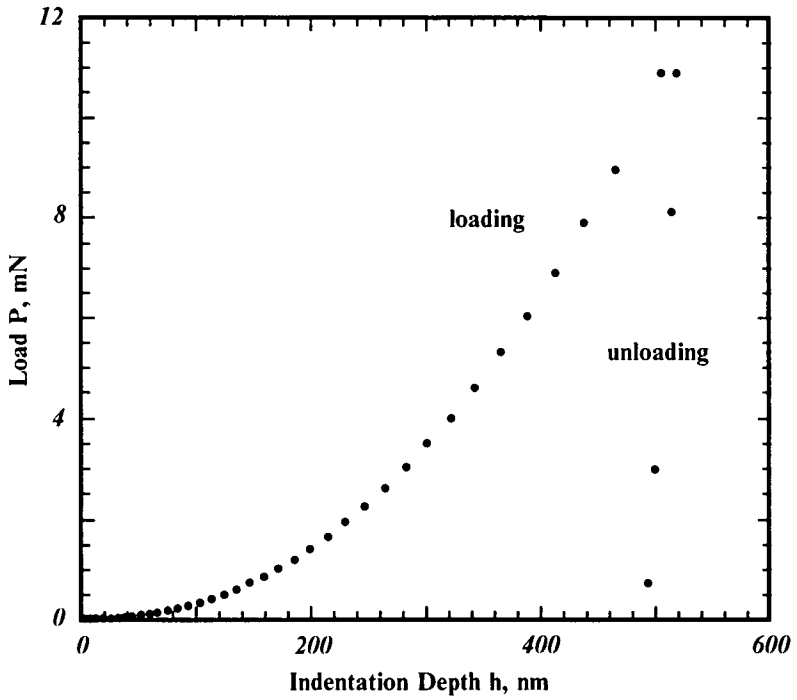

Figure 6. Load–displacement record from an instrumented indentation test.

The expressions for both elastic modulus and hardness contain the contact area, which is correlated to the indentation depth both theoretically, through the known geometry of the indenter, and experimentally, by indenting a material with known elastic modulus. This tip calibration procedure consists of indenting a standard material (often fused quartz or single crystal Al) to various maximum indentation depths. Since the contact area is determined from tip calibration, various tip geometries can be used, with the most common being the Berkovich three-sided pyramid geometry. From the manufacturing standpoint, a three-sided pyramid always ends as a point, and the tip radius can be as sharp as 10–50 nm. Other geometries are also used, and include Vickers (a standardized square pyramid), cube corner, conical and wedge indenters. The unloading slope, dP/dh is related to the tip geometry as

$$\frac{dP}{dh} = 2\beta\sqrt{\frac{A}{\pi}}E_r \tag{4}$$

where h is the indentation depth, and β is a constant, near unity, for a given tip geometry. King *et al.* calculated β values for different tip geometries using finite element analysis.[17] One should note that the tip calibration does not account for either plastic pile-up or sink-in of both the standard and the specimen materials, which causes inaccuracies in indentation depth and contact area determination. In addition, the total test compliance, i.e., the inverse of stiffness, is affected by the indentation contact. One should also account for the test frame compliance, C_f, as it offsets the total test compliance:

$$C_{total} = C_f + \frac{\sqrt{\pi}}{2\sqrt{A}E} \tag{5}$$

In order to avoid substrate effects on the measured mechanical properties, a film should be indented only up to a certain percentage of its thickness (up to 10–20%). There is also an influence of the residual stress and substrate effects that are hard to account for in the analysis.[18,19] Indentation curve analysis has been extended in the past few years with new finite-element-based models being developed.[20,21]

A comprehensive review of the method applied for magnetic storage and MEMS materials was reported by Li and Bhushan.[22]

2.3. OTHER TECHNIQUES

2.3.1. *Wafer curvature*

The basic principle of the wafer curvature technique is that differential thermal expansion between a specimen film and a silicon substrate produce measurable curvature of the substrate (the wafer); the curvature is related directly to the product of stress and thickness in the film through the Stoney equation.[23,24] This phenomenon is used in evaluating and adjusting film deposition procedures, to measure residual stress in the deposited films. High values of residual stress, especially tension, may make a film less resistant to delamination from the substrate.

Wafer curvature measurement was adapted for characterization of mechanical behavior by Nix.[25] The substrate with its film is placed in a furnace equipped for measurement of the substrate curvature. The temperature is cycled, while the curvature is recorded. Given the film thickness, the film stress can be plotted against temperature. The accessible range of temperature is limited only by the eventual breakdown of the specimen film by melting or chemical reaction. The stress depends in turn on the difference in thermal

expansion between the specime
constants of the specimen filn
temperature imply plastic deforr
this deformation is confirmed by
first temperature cycle. The adv
include the simplicity (in princip
the specimen, which is a film o
factured products, without the n
strate beneath the film. Analysis
knowledge of the elastic properti
substrate. The disadvantage is that
to failure cannot be measured, anc
modulus, flow stress, and tempera
very successful in providing insi
particularly in aluminum films.[25]

2.3.2. *Pressurized bulge testing*

The name of the bulge test is d
beneath a region of the specimen
pressurized fluid introduced bene
surized membrane can be used to
of the pressurized region is chose
square, and rectangular shapes ha
mation of the membrane can b
optical techniques. This technique
thin films; care must be taken to p
film, including the possibility of
been used to measure the adhesion

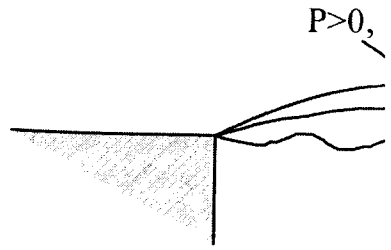

Figure 7. Schematic diagram of the bulge
(zero pressure), infinitesimal, and finite pr

is a constant, near unity, for a
β values for different tip geo-
hould note that the tip calibration
or sink-in of both the standard
naccuracies in indentation depth
ı, the total test compliance, i.e.,
indentation contact. One should
, C_f, as it offsets the total test

$$\frac{\sqrt{\pi}}{\sqrt{A}E} \qquad (5)$$

neasured mechanical properties,
n percentage of its thickness (up
he residual stress and substrate
analysis.[18,19] Indentation curve
years with new finite-element-

l applied for magnetic storage
l Bhushan.[22]

: technique is that differential
and a silicon substrate produce
wafer); the curvature is related
; in the film through the Stoney
evaluating and adjusting film
stress in the deposited films.
ension, may make a film less

apted for characterization of
:e with its film is placed in a
rate curvature. The temperature
ven the film thickness, the film
accessible range of temperature
the specimen film by melting
ırn on the difference in thermal

expansion between the specimen film and the substrate, and the elastic constants of the specimen film. Deviations from linear behavior with temperature imply plastic deformation of the specimen film; the nature of this deformation is confirmed by the hysteresis loop observed at least on the first temperature cycle. The advantages of the wafer curvature technique include the simplicity (in principle) of both the experimental technique and the specimen, which is a film on the same substrate used in actual manufactured products, without the necessity of selectively removing the substrate beneath the film. Analysis of the results using Eq. (1) does not require knowledge of the elastic properties of the deposited film, only those of the substrate. The disadvantage is that the ultimate tensile strength and elongation to failure cannot be measured, and that only certain combinations of Young's modulus, flow stress, and temperature are accessible. This technique has been very successful in providing insight and data on deformation mechanisms, particularly in aluminum films.[25]

2.3.2. *Pressurized bulge testing*

The name of the bulge test is descriptive: by etching away the substrate beneath a region of the specimen film, the film can be exposed to stress by a pressurized fluid introduced beneath the substrate. The mechanics of a pressurized membrane can be used to analyze the observed behavior. The shape of the pressurized region is chosen based on the purpose of the test; circular, square, and rectangular shapes have been explored. The out-of-plane deformation of the membrane can be measured by interferometry or related optical techniques. This technique has been used to explore the elasticity of thin films; care must be taken to properly characterize the initial state of the film, including the possibility of residual stress,[26,27] Figure 7. It has also been used to measure the adhesion between the film and the substrate.[28]

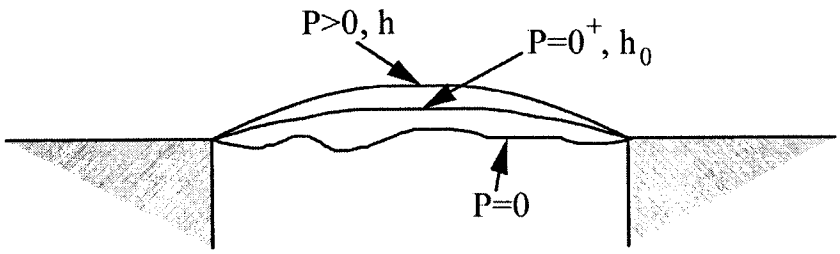

Figure 7. Schematic diagram of the bulge test specimen, showing stages in the loading: slack (zero pressure), infinitesimal, and finite pressure.

2.3.3. *Deformed and Resonant Cantilever*

Micromachined cantilevers have been used as specimens in thin film properties measurements.[29,30] Photolithography can be used to define the cantilever geometry. Cantilevers can be deformed by loading with, for example, an instrumented indenter, or can be excited to resonance, to measure film elastic properties. The relationship between the mechanical stiffness or the resonant frequency and the elastic constant of the film depends sensitively on the dimensions of the cantilever.[31] The ideas of the bulge test and resonance can be combined in the resonant membrane test, which can be used to determine the product of film elastic modulus and mass per unit area. If the thickness and mass density of the film are known, the elastic modulus can be measured.

3. Adhesion tests based on fracture mechanics

Adhesion between layers of different materials is a critical issue in microelectronic packages, and also within the chips themselves. While the time-honored "scotch tape" adhesion test is still in use, quantitative tests, developed in recent years based on the concepts of fracture mechanics, provide material characteristics that can be compared to calculable stress- and strain-based driving forces, and are therefore suitable for use in lifetime predictions.[32] Reviews by Volinsky et al.[33] and by Lane[34] provide useful summaries. The basic idea, as in macroscale fracture mechanics, is that it is useful to quantify the conditions under which an existing crack may advance. The crack, in this case, is assumed to be a small delamination of the film from the substrate. The driving force for crack propagation is taken as the strain energy release rate, which depends on the geometry and the stress state.

3.1. FRACTURE MECHANICS FOR DELAMINATION

Both tensile and compressive stresses in thin films promote adhesion failures; a thin film in compression buckles, delaminates and spalls from the substrate when its strain energy release rate exceeds a critical value that is characteristic of the adhesion between film and substrate.[35] A general, simplified form of the strain energy release rate, G, in a stressed film, regardless of the algebraic sign of the stress is

$$G = Z\frac{\sigma_f^2 h}{E_f}, \qquad (6)$$

where σ_f is the stress in the film
modulus of elasticity, and Z is a c
accurately, the energy release rate
isolated crack is

$$G = g(\alpha,$$

where $g(\alpha,\beta)$ is a function of th
be found in.[36,37] This strain energ
fracture. Film fracture or delamina
release rate exceeds the toughness c
ness, Γ_f respectively ($G > G_f$, or
failures by either reducing the film
adhesion. Practically, the film thic
stress level, there is a certain criti
observed. As an example, Figure
low-k dielectric film 2 μm thick. Tl
If a film has fractured, and if its r
Eqs. (6) and (7) can be used as uppe

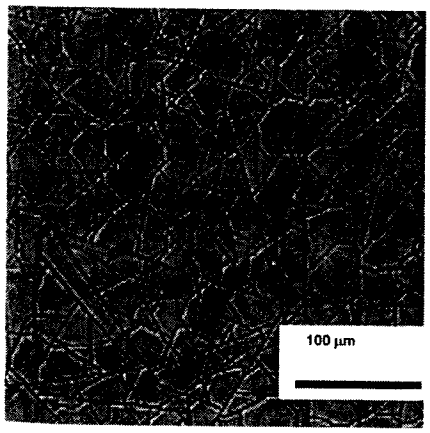

Figure 8. Optical and AFM image

In the case of compressed f
commonly observed (Figure 9). The
asses thin film adhesion. The follo
and Suo's developments for buckli
Upon buckling, the stress in the film

d as specimens in thin film pro-
/ can be used to define the canti-
ed by loading with, for example,
:d to resonance, to measure film
n the mechanical stiffness or the
t of the film depends sensitively
ideas of the bulge test and reso-
nbrane test, which can be used to
lus and mass per unit area. If the
known, the elastic modulus can

:hanics

:rials is a critical issue in micro-
ıips themselves. While the time-
ı use, quantitative tests, developed
:ture mechanics, provide material
ılculable stress- and strain-based
for use in lifetime predictions.[32]
[4] provide useful summaries. The
ıics, is that it is useful to quantify
ack may advance. The crack, in
nation of the film from the sub-
tion is taken as the strain energy
y and the stress state.

/INATION

n thin films promote adhesion
, delaminates and spalls from the
:e exceeds a critical value that is
ilm and substrate.[35] A general,
ıse rate, G, in a stressed film,
; is

$$\frac{^2 h}{_f}, \qquad (6)$$

/

where σ_f is the stress in the film, h is the film thickness, E_f is the modulus of elasticity, and Z is a dimensionless cracking parameter. More accurately, the energy release rate averaged over the front of advancing isolated crack is

$$G = g(\alpha,\beta)\frac{\pi(1-\nu^2)\sigma_f^2 h}{2E_f} \qquad (7)$$

where $g(\alpha,\beta)$ is a function of the Dundurs parameters α and β, and can be found in.[36,37] This strain energy release rate is the driving force for fracture. Film fracture or delamination is observed when the strain energy release rate exceeds the toughness of the film, G_f, or the interfacial toughness, Γ_I respectively ($G > G_f$, or $G > \Gamma_I$). One can avoid these types of failures by either reducing the film thickness, or the stress, or by increasing adhesion. Practically, the film thickness is easier to control. For a given stress level, there is a certain critical film thickness at which failures are observed. As an example, Figure 8 shows through-thickness cracks in a low-k dielectric film 2 μm thick. Thinner films showed no signs of failure. If a film has fractured, and if its residual stress and thickness are known, Eqs. (6) and (7) can be used as upper bound estimates for adhesion.

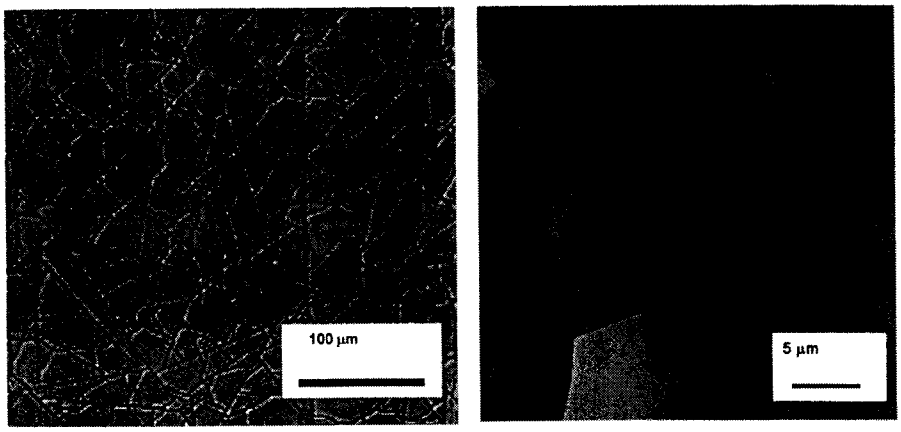

Figure 8. Optical and AFM images of cracks in low-k dielectric thin film.

In the case of compressed films, telephone cord delamination is commonly observed (Figure 9). The geometry of the buckles can be used to asses thin film adhesion. The following analysis is based on Hutchinson's and Suo's developments for buckling-driven delamination of thin films.[35] Upon buckling, the stress in the film, σ_B, is estimated as

$$\sigma_B = \frac{\pi^2}{12}\frac{E}{(1-\nu^2)}\left(\frac{h}{b}\right)^2 \tag{8}$$

where h is the film thickness, b is the blister half-width, and E and ν are Young's modulus and Poisson's ratio, respectively. The buckling stress acts in the vertical direction. The compressive residual stress, σ_r, responsible for producing buckling delamination is

$$\sigma_r = \frac{3}{4}\sigma_B\left(\frac{\delta^2}{h^2}+1\right) \tag{9}$$

where δ is the blister height. The film steady state interfacial toughness in the direction of blister propagation (Figure 10a) can be estimated as

$$\Gamma_{SS} = \frac{(1-\nu^2)h\sigma_r^2}{2E}\left(1-\frac{\sigma_B}{\sigma_r}\right)^2 \tag{10}$$

Mode-dependent interfacial toughness in the buckling direction, perpendicular to blister propagation is:

$$\Gamma(\Psi) = \frac{(1-\nu^2)h}{2E}(\sigma_r-\sigma_B)(\sigma_r+3\sigma_B) \tag{11}$$

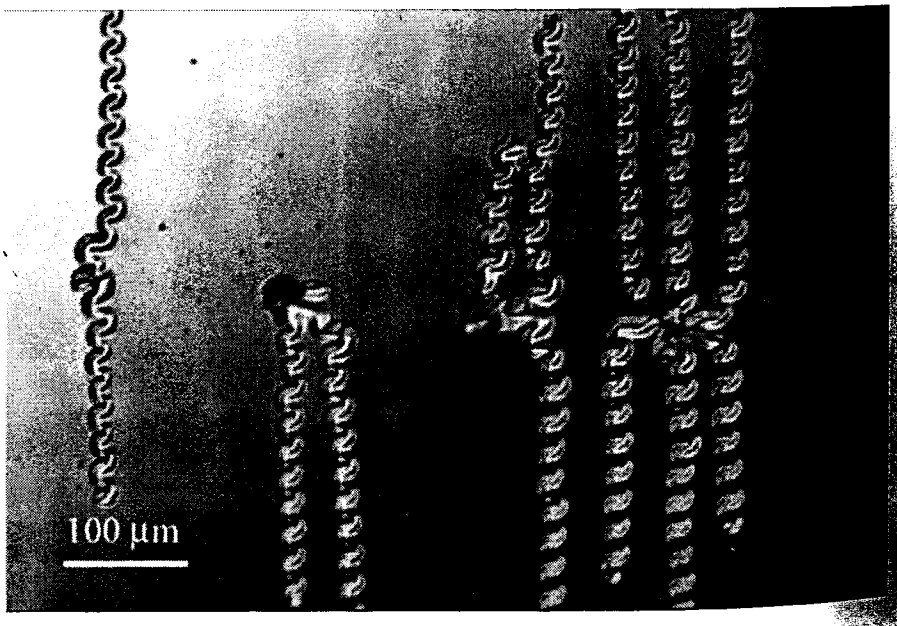

Figure 9. Telephone cord delamination in a 1 μm tungsten film.

3.2. SUPERLAYER TEST WITH

The superlayer indentation test
at the microscale. A superlayer
and high adhesion, is deposited
used to initiate delamination. Tl
additional driving force for in
plastic deformation of the teste
tip is pressed against the superla
necessary for crack initiation and
optically (Figure 10a). The inde
depth of the load–displacement
Both the blister radius and the in
the strain energy release rate (n
Calculations for adhesion measur
developed by Marshall and Evan
Gerberich for multilayer films.[39,
blister seen from making indent
load and a corresponding load–
plastic indentation depth is obta
65% of the unloading curve,[16] an
based on the tip geometry. It is
plastic deformation around the in
the crack tip, allowing calculatic
the strain energy release rate, a
Adhesion results for several m
summarized in.[41]

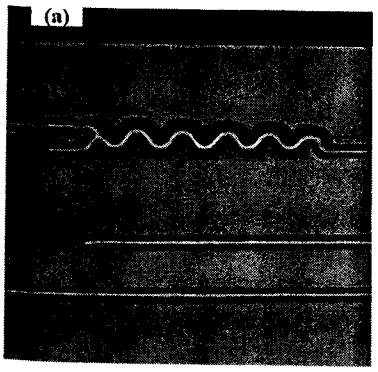

Figure 10. Analysis of the telephone-c
previous figure. (a) Telephone cord dela
diamond-like carbon (DLC) film on Si. (

$$\frac{E}{1-\nu^2)}\left(\frac{h}{b}\right)^2 \tag{8}$$

: blister half-width, and E and ν are
respectively. The buckling stress acts
sive residual stress, σ_r, responsible

$$_B\left(\frac{\delta^2}{h^2}+1\right) \tag{9}$$

steady state interfacial toughness in
ure 10a) can be estimated as

$$\frac{h\sigma_r^2}{}\left(1-\frac{\sigma_B}{\sigma_r}\right)^2 \tag{10}$$

ıess in the buckling direction, per-

$$_r-\sigma_B)(\sigma_r+3\sigma_B) \tag{11}$$

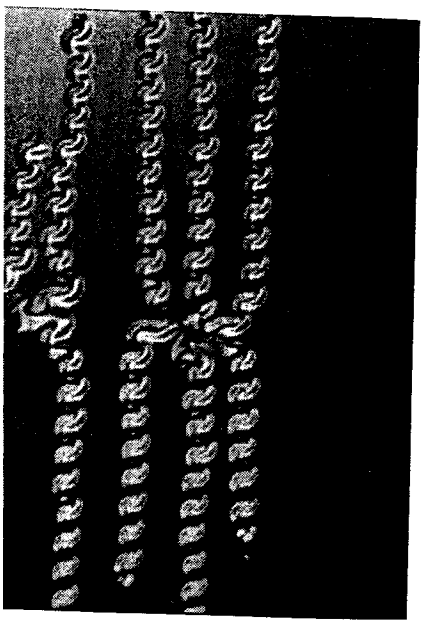

ion in a 1 μm tungsten film.

3.2. SUPERLAYER TEST WITH INDENTATION

The superlayer indentation test provides information on local film adhesion at the microscale. A superlayer film, selected for high stress, high strength, and high adhesion, is deposited on top of the film to be tested. Indentation is used to initiate delamination. The highly stressed hard superlayer provides additional driving force for interfacial crack propagation, and prevents plastic deformation of the tested film around the indenter. As the indenter tip is pressed against the superlayer film stack, it supplies additional energy necessary for crack initiation and propagation. The blister radius is measured optically (Figure 10a). The indentation volume is obtained from the plastic depth of the load–displacement curve (Figure 10b) and the tip geometry. Both the blister radius and the indentation volume are then used to calculate the strain energy release rate (measure of the practical work of adhesion). Calculations for adhesion measurements were made by following the solution developed by Marshall and Evans[38] that was further expanded by Kriese and Gerberich for multilayer films.[39,40] Figure 11a shows a typical delamination blister seen from making indents with a conical tip at 300 mN maximum load and a corresponding load–displacement curve. From Figure 11b, the plastic indentation depth is obtained by using the power law fit of the top 65% of the unloading curve,[16] and used to calculate the indentation volume, based on the tip geometry. It is assumed that the volume is conserved, and plastic deformation around the indenter results in the elastic displacement at the crack tip, allowing calculation of the indentation stress, and ultimately the strain energy release rate, a measure of the practical work of adhesion. Adhesion results for several microelectronics-relevant film materials are summarized in.[41]

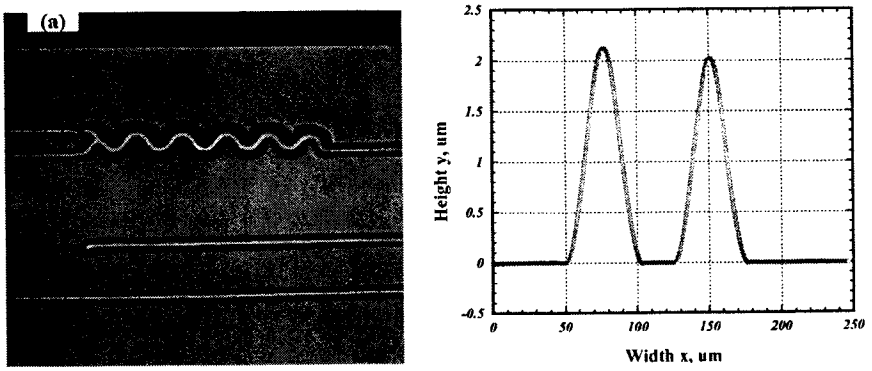

Figure 10. Analysis of the telephone-cord delamination of a tungsten film shown in the previous figure. (a) Telephone cord delamination in a 1 μm tungsten film on top of a 2 nm diamond-like carbon (DLC) film on Si. (b) Corresponding blister heights profile.

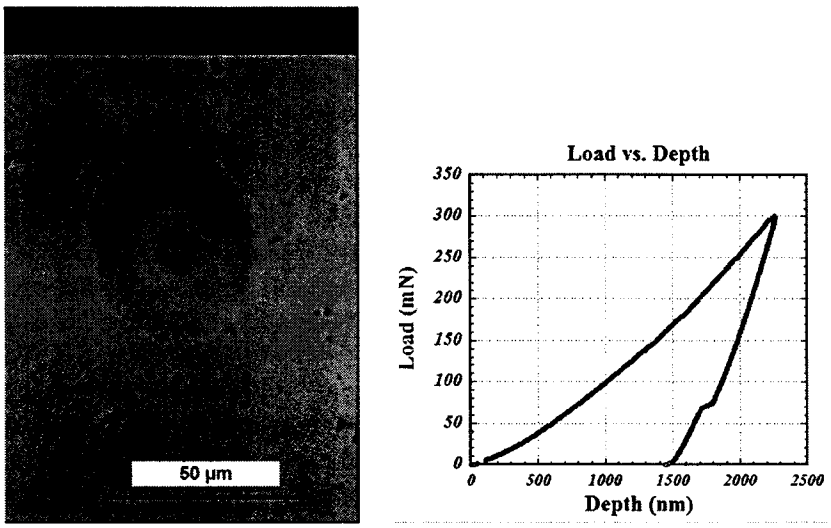

Figure 11. (a) Indentation-induced delamination blister in tungsten film; and (b) corresponding load–displacement curve.

3.3. FOUR-POINT-BEND TEST FOR THIN FILM ADHESION

Because the interfacial energies found in films are numerically much lower than those in bulk metals, for which fracture toughness testing was developed, the four-point-bend bar with a cracks propagating along its length from a central notch has been found useful.[32,42–44] Below, we briefly describe this technique, to show a specific application of fracture mechanics in thin film adhesion. The many reports of adhesion measurement methods in the literature testify to the importance of the problem, the difficulty of the measurement, and the ingenuity of the researchers, but a detailed review is beyond the scope of this article.

The delaminating beam test specimen, Figure 12, is a four-point-bend bar with an interface of interest built into the interior of the beam along the whole length. A "sandwich" beam made with the substrate on the top and bottom, and the surface layers bonded together in the center, is a typical geometry. The substrate layers are much thicker than the interface layer, and give the assembly sufficient stiffness to handle. In the bending beam, the outer fiber in tension is often located on the upper side, and is conventionally referred to as the top of the specimen. The bottom fiber is in compression. The top section is carefully cut without notching the bottom section. Cracks are intentionally nucleated to grow away from the notch along the interface layer being tested. While the crack length significantly exceeds the thickness of the cut layer, the energy release rate is constant until the cracks reach the inner loading points of the four-point-bend specimen.

The energy release rate is evalı
cimen geometry, and elastic proj
An advantage of this test is tl
adhesion do not include the r
difficult to measure. Becker[44] p
specimen may depend on the s
standardized fracture toughness
serious disadvantage for testing
because actual-size specimens c

All the fracture toughness te
design of electronic packages a
such as polymer-metal interfa
around 10 J/m^2.

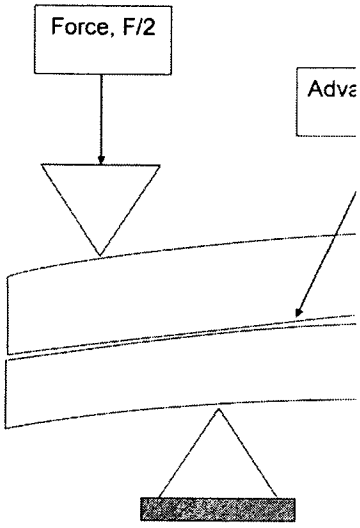

Figure 12. Delaminating beam specim
adhesive interface.

4. A new development: electr

It has been proposed that the cyc
joule heating by AC (alternating
in conductive films on silicon s
mechanical reliability of thin fi
electrical test to extract informat
connect structures because of the

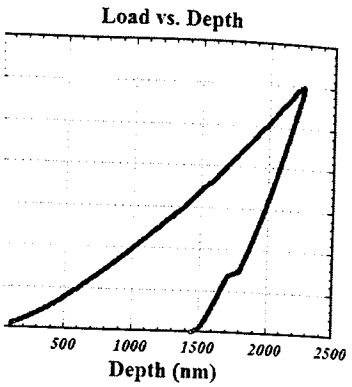

r in tungsten film; and (b) corresponding

'ILM ADHESION

lms are numerically much lower
toughness testing was developed,
agating along its length from a
Below, we briefly describe this
fracture mechanics in thin film
asurement methods in the litera-
he difficulty of the measurement,
detailed review is beyond the

Figure 12, is a four-point-bend
e interior of the beam along the
ith the substrate on the top and
ther in the center, is a typical
nicker than the interface layer,
handle. In the bending beam,
on the upper side, and is con-
ecimen. The bottom fiber is in
it without notching the bottom
to grow away from the notch
the crack length significantly
energy release rate is constant
f the four-point-bend specimen.

The energy release rate is evaluated from the load and displacement, specimen geometry, and elastic properties of the support layers of the specimen. An advantage of this test is that the parameters needed to evaluate the adhesion do not include the residual stress on the film, which may be difficult to measure. Becker[44] points out that properties measured with this specimen may depend on the specific geometry, contrary to the case for standardized fracture toughness specimens. This is not considered to be a serious disadvantage for testing materials for chips and electronic packages, because actual-size specimens can be tested.

All the fracture toughness techniques highlight a critical problem in the design of electronic packages and chips: some commonly used interfaces, such as polymer-metal interfaces, have very low fracture toughness,[32] around 10 J/m^2.

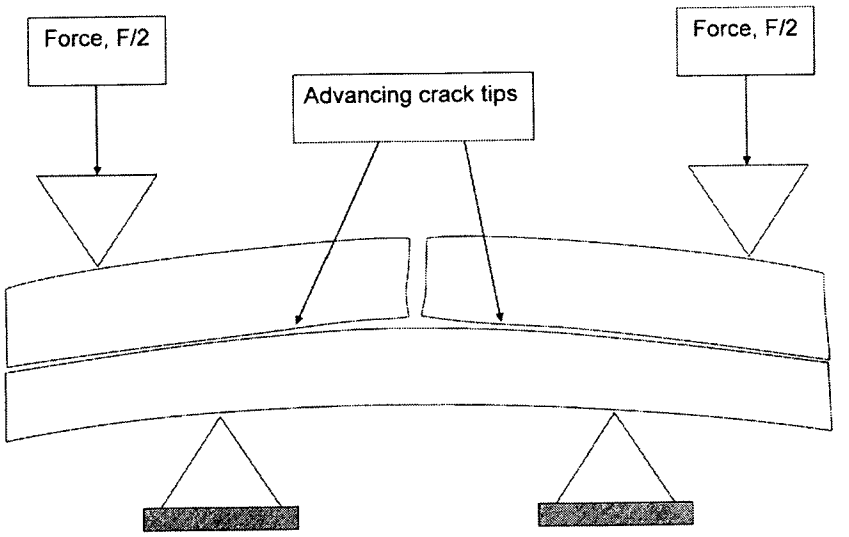

Figure 12. Delaminating beam specimen for measuring the energy required to separate an adhesive interface.

4. A new development: electrical testing for mechanical reliability

It has been proposed that the cyclic stresses produced by the combination of joule heating by AC (alternating current) and differential thermal expansion in conductive films on silicon substrates may be useful in evaluating the mechanical reliability of thin films. Interest has arisen in the use of this electrical test to extract information about the mechanical behavior of interconnect structures because of the problems associated with more conventional

approaches to mechanical characterization of very small thin-film structures. Microtensile testing requires special test structures, which must become much more sophisticated as the linewidth of interest falls below 1 μm. Nanoindentation with conventional indenter shapes requires an area of at least a few square micrometers. The use of atomic force microscopy to extract mechanical properties is in its infancy. And all of these require that the film to be tested be exposed; none are applicable to buried lines. On the other hand, interconnect lines within the damascene structure are commonly tested electrically during development of advanced interconnect designs by industry. So a further development of electrical testing, to a point where it could produce mechanical information about narrow, buried lines or about other small, inaccessible structures, would be a significant advance.

The AC fatigue test technique[45] uses cyclic Joule heating to apply thermal cycles to metal lines and vias in damascene dielectric structures on silicon substrates. Cyclic stresses from differential thermal expansion produce elastic and possibly plastic deformation in the metal line and its surrounding dielectric. The use of high-amplitude, low-frequency alternating current in tests of thin-film copper lines was explored by Mönig et al.[45]; they reported surface topography changes that appeared to be mechanical in origin. Tests of aluminum lines under by AC fatigue produced topographic damage in the form of regular undulations or wrinkles.[46] Extensive TEM and SEM examination of these aluminum lines revealed that the AC stressing produced dislocations, grain growth, and grain rotation in various regions of the specimen.[47,48]

Barbosa et al. plotted the behavior of aluminum lines under AC stress as S-N curves, familiar from metal fatigue.[49] They showed that their data could be fit by the Basquin law for fatigue in the appropriate range of cyclic temperature, and that the values of the exponent in the fit were within the same range as those for mechanical fatigue of bulk metals. The stress prefactor in the Basquin law is an estimator of the ultimate tensile strength in metals; they proposed this same relationship for the AC fatigue test. They were able to deduce a value of this stress prefactor that agreed with the ultimate tensile strength for their thin film, as measured by the microtensile test.[49] AC fatigue data for copper and aluminum films on substrates appear consistent with conventional mechanical fatigue tests where the temperature reached in the AC fatigue test is not too high (R.R. Keller, 2008, Personal communication). Figure 13 shows mechanical fatigue data from the literature plotted for comparison with AC fatigue data. The stresses for the AC data points were calculated using the simple biaxial stress formula. For both the copper and the aluminum data in this figure, the AC data are offset vertically from the bulk data, indicating different values of the fatigue stress prefactors in the Basquin fits to the data sets. We ascribe these differences

to the difference in grain sizes betw
other effects, such as crystallograp
nical constraint by the substrate, r
the bulk materials are noted on the
diameters of less than 1 μm.

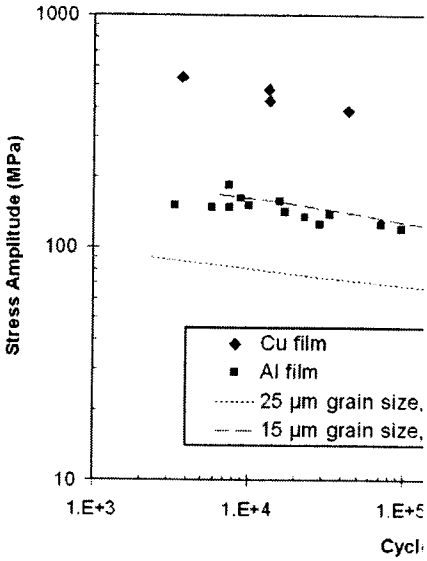

Figure 13. Fatigue stress vs lifetime data p
data from mechanical fatigue tests and rec
shows similar behavior for all cases. The
grain sizes and possibly other differences
text.

5. Conclusion

The state of the art of measurement
has advanced significantly in the pas
films, with thicknesses of 0.5 μm
tens of micrometers, are made routi
properties of these micrometer-scal
Hall–Petch relation. Fracture of the
problem of general relevance, but fi
the appropriate framework for quar
film-to-substrate adhesion. Some
adhesion have been described. Nano
latest new challenge in understa
behavior of materials.

n of very small thin-film structures.
st structures, which must become
idth of interest falls below 1 μm.
enter shapes requires an area of at
f atomic force microscopy to extract
nd all of these require that the film
cable to buried lines. On the other
cene structure are commonly tested
ed interconnect designs by industry.
testing, to a point where it could
narrow, buried lines or about other
significant advance.
yclic Joule heating to apply thermal
ene dielectric structures on silicon
l thermal expansion produce elastic
e metal line and its surrounding
w-frequency alternating current in
ed by Mönig et al.[45]; they reported
l to be mechanical in origin. Tests
produced topographic damage in
kles.[46] Extensive TEM and SEM
vealed that the AC stressing pro-
ain rotation in various regions of

luminum lines under AC stress as
They showed that their data could
the appropriate range of cyclic
xponent in the fit were within the
ue of bulk metals. The stress pre-
of the ultimate tensile strength in
hip for the AC fatigue test. They
ss prefactor that agreed with the
, as measured by the microtensile
minum films on substrates appear
atigue tests where the temperature
high (R.R. Keller, 2008, Personal
cal fatigue data from the literature
ata. The stresses for the AC data
axial stress formula. For both the
ure, the AC data are offset ver-
erent values of the fatigue stress
ets. We ascribe these differences

to the difference in grain sizes between the bulk and the thin film materials; other effects, such as crystallographic texture and effects of added mechanical constraint by the substrate, may also play a role. The grain sizes for the bulk materials are noted on the plot; the thin films have average grain diameters of less than 1 μm.

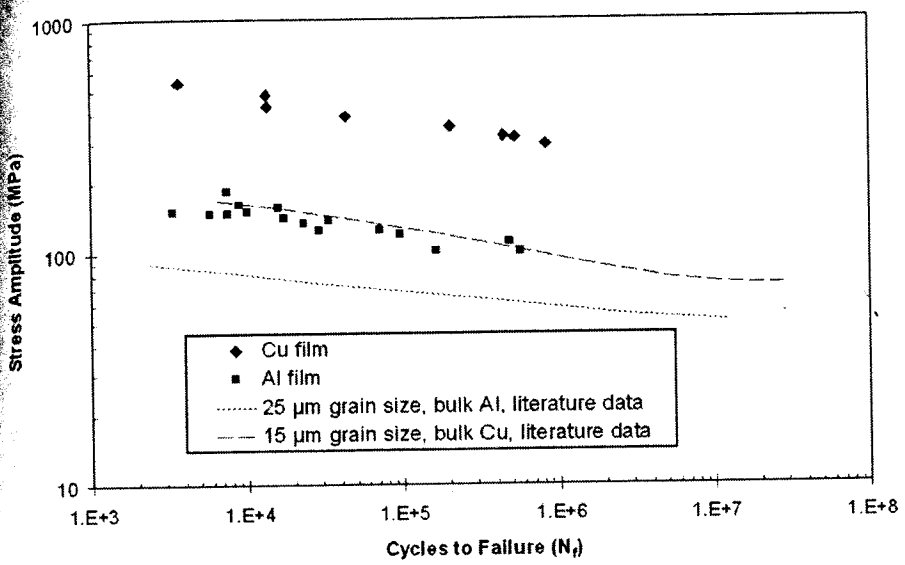

Figure 13. Fatigue stress vs lifetime data plotted as S-N curves. The plot includes literature data from mechanical fatigue tests and recent data obtained with the AC fatigue test, and shows similar behavior for all cases. The vertical offsets are a result of differences in the grain sizes and possibly other differences between bulk and film materials as noted in the text.

5. Conclusion

The state of the art of measurements of mechanical properties for thin films has advanced significantly in the past 20 years. Measurements of microscale films, with thicknesses of 0.5 μm and above, and in-plane dimensions of tens of micrometers, are made routinely by multiple techniques. The tensile properties of these micrometer-scale films can be understood by use of the Hall–Petch relation. Fracture of the films themselves has not proved to be a problem of general relevance, but fracture mechanics has been found to be the appropriate framework for quantitative treatment of layer-to-layer and film-to-substrate adhesion. Some of the tests now in use for interfacial adhesion have been described. Nanometer-scale materials now represent the latest new challenge in understanding and measuring the mechanical behavior of materials.

References

1. Read, D. T.; Volinsky, A. A. Thin Films for Microelectronics and Photonics: Physics, Mechanics, Characterization, and Reliability, in *Materials and Structures: Physics, Mechanics, Design, Reliability, Packaging: Volume 1 Materials Physics/Materials Mechanics.*, Suhir, E.; Lee, Y. C.; Wong, C. P., editors; Springer: New York, 2007; Chapter 4, pp. 135–180.
2. Brotzen, F. R. Mechanical Testing of Thin-Films, International Materials Reviews 39 (1), 24–45, 1994.
3. Ding, X. Y.; Ko, W. H.; Mansour, J. M. Residual-Stress and Mechanical-Properties of Boron-Doped P+-Silicon Films, Sensors and Actuators A-Physical 23 (1–3), 866–871, 1990.
4. Read, D. T.; Dally, J. W. A New Method for Measuring the Strength and Ductility of Thin-Films, Journal of Materials Research 8 (7), 1542–1549, 1993.
5. Sharpe, W. N.; Jackson, K. M.; Coles, G.; Eby, M. A.; Edwards, R. L. Tensile Tests of Various Thin Films, in *ASTM STP 1413: Mechanical Properties of Structural Films;* edited by Muhlstein, C.; Brown, S. B., editors; American Society for Testing and Materials: West Conshohoken, PA, 2001; pp. 229–247.
6. Read, D. T. Young's Modulus of Thin Films by Speckle Interferometry, Measurement Science and Technology 9 (4), 676–685, 1998.
7. Sharpe, W. N.; Yuan, B.; Edwards, R. L. A New Technique for Measuring the Mechanical Properties of Thin Films, Journal of Microelectromechanical Systems 6 (3), 193–199, 1997.
8. Read, D. T.; Cheng, Y. W.; Keller, R. R.; McColskey, J. D. Tensile Properties of Free-Standing Aluminum Thin Films, Scripta Materialia 45 (5), 583–589, 2001.
9. Ruud, J. A.; Josell, D.; Spaepen, F.; Greer, A. L. A New Method for Tensile Testing of Thin Films, Journal of Materials Research 8 (1), 112–117, 1993.
10. Espinosa, H. D.; Prorok, B. C.; Peng, B. Plasticity Size Effects in Free-Standing Submicron Polycrystalline FCC Films Subjected to Pure Tension, Journal of the Mechanics and Physics of Solids 52 (3), 667–689, 2004.
11. Haque, M. A.; Saif, M. T. A. Deformation Mechanisms in Free-Standing Nanoscale Thin Films: A Quantitative in situ Transmission Electron Microscope Study, Proceedings of the National Academy of Sciences of the United States of America 101 (17), 6335–6340, 2004.
12. LaVan, D. A.; Tsuchiya, T.; Coles, G.; Knauss, W. G.; Chasiotis, I.; Read, D. T. Cross Comparison of Direct Strength Testing Techniques on Polysilicon Films, in *ASTM STP 1413: Mechanical Properties of Structural Films*; edited by Muhlstein, C.; Brown, S. B., editors; American Society for Testing and Materials: West Conshohoken, PA, 2001; pp. 16–27.
13. VanLandingham, M. R. Review of Instrumented Indentation, Journal of Research of the National Institute of Standards and Technology 108 (4), 249–265, 2003.
14. Loubet, J. L.; Georges, J. M.; Marchesini, O.; Meille, G. Vickers Indentation Curves of Magnesium-Oxide (MgO), Journal of Tribology-Transactions of the ASME 106 (1), 43–48, 1984.
15. Doerner, M. F.; Nix, W. D. A Method for Interpreting the Data from Depth-Sensing Indentation Measurements, Journal of Materials Research 1 (4), 601–616, 1986.
16. Oliver, W. C.; Pharr, G. M. An Improved Technique for Determining Hardness and Elastic-Modulus Using Load and Displacement Sensing Indentation Experiments, Journal of Materials Research 7 (6), 1564–1583, 1992.

17. King, R. B.; Osullivan, T. C. Slidin Elastic Half-Space, International Jou
18. Tsui, T. Y.; Oliver, W. C.; Pharr, (Mechanical Properties Using Nanoin Alloy, Journal of Materials Research
19. Bolshakov, A.; Oliver, W. C.; Pharr, Mechanical Properties Using Nanoin Materials Research 11 (3), 760–768,
20. Hainsworth, S. V.; Chandler, H. W Displacement Loading Curves, Journ
21. Berriche, R. Vickers Hardness from I (4), 617–620, 1995.
22. Li, X. D.; Bhushan, B. A Review of] Technique and Its Applications, Mate
23. Freund, L. B.; Suresh, S. *Thin Film Evolution*; Cambridge University Pre
24. Ohring, M. *Materials Science of Thir* San Diego, CA, 2002.
25. Nix, W. D. Mechanical-Properties of Metallurgy and Materials Science 20
26. Jankowski, A. F.; Tsakalakos, T. Eff Enhanced Modulus in Multilayered F
27. Small, M. K.; Nix, W. D. Analysis of Mechanical-Properties of Thin-Films 1992.
28. Liechti, K. M.; Shirani, A. Large-S Journal of Fracture 67 (1), 21–36, 199
29. Petersen, K. E.; Guarnieri, C. R. Yo Micromechanics, Journal of Applied I
30. Osterberg, P. M.; Senturia, S. D. M- Measurement Using Electrostatically mechanical Systems 6 (2), 107–118, 1
31. Weihs, T. P.; Hong, S.; Bravman, J. C Microbeams – A New Technique for Journal of Materials Research 3 (5), 9
32. Dauskardt, R.; Lane, M.; Ma, Q.; Kri Thin Film Structures, Engineering Fra
33. Volinsky, A. A.; Moody, N. R.; Gerb for Thin Films on Substrates, Acta Ma
34. Lane, M. Interface Fracture, Annual R
35. Thouless, M. D. Cracking and Delan and Technology A-Vacuum Surfaces
36. Hutchinson, J. W.; Suo, Z. Mixed-M Applied Mechanics, 29, 63–191, 1992
37. Beuth, J. L. Cracking of Thin Bonde of Solids and Structures 29 (13), 1657-
38. Marshall, D. B.; Evans, A. G. Measu Films by Indentation .1. Mechanics Physics 56 (10), 2632–2638, 1984.

ns for Microelectronics and Photonics: Physics.
ability, in *Materials and Structures: Physics.*
iging: Volume 1 Materials Physics/Materials
ng, C. P., editors; Springer: New York, 2007;

Thin-Films, International Materials Reviews 39

. Residual-Stress and Mechanical-Properties of
and Actuators A-Physical 23 (1–3), 866–871,

)d for Measuring the Strength and Ductility of
1 8 (7), 1542–1549, 1993.
.; Eby, M. A.; Edwards, R. L. Tensile Tests of
Mechanical Properties of Structural Films;
, editors; American Society for Testing and
pp. 229–247.
ilms by Speckle Interferometry, Measurement
998.
. L. A New Technique for Measuring the
nal of Microelectromechanical Systems 6 (3),

McColskey, J. D. Tensile Properties of Free-
aterialia 45 (5), 583–589, 2001.
, A. L. A New Method for Tensile Testing of
3 (1), 112–117, 1993.
B. Plasticity Size Effects in Free-Standing
ubjected to Pure Tension, Journal of the
7–689, 2004.
Mechanisms in Free-Standing Nanoscale Thin
Electron Microscope Study, Proceedings of
ited States of America 101 (17), 6335–6340,

uss, W. G.; Chasiotis, I.; Read, D. T. Cross
hniques on Polysilicon Films, in *ASTM STP*
Films; edited by Muhlstein, C.; Brown, S. B.,
laterials: West Conshohoken, PA, 2001; pp.

nted Indentation, Journal of Research of the
gy 108 (4), 249–265, 2003.
.; Meille, G. Vickers Indentation Curves of
)logy-Transactions of the ASME 106 (1),

Interpreting the Data from Depth-Sensing
ls Research 1 (4), 601–616, 1986.
Technique for Determining Hardness and
ement Sensing Indentation Experiments,
3, 1992.

17. King, R. B.; Osullivan, T. C. Sliding Contact Stresses in A Two-Dimensional Layered Elastic Half-Space, International Journal of Solids and Structures 23 (5), 581–597, 1987.
18. Tsui, T. Y.; Oliver, W. C.; Pharr, G. M. Influences of Stress on the Measurement of Mechanical Properties Using Nanoindentation .1. Experimental Studies in an Aluminum Alloy, Journal of Materials Research 11 (3), 752–759, 1996.
19. Bolshakov, A.; Oliver, W. C.; Pharr, G. M. Influences of Stress on the Measurement of Mechanical Properties Using Nanoindentation .2. Finite Element Simulations, Journal of Materials Research 11 (3), 760–768, 1996.
20. Hainsworth, S. V.; Chandler, H. W.; Page, T. F. Analysis of Nanoindentation Load-Displacement Loading Curves, Journal of Materials Research 11 (8), 1987–1995, 1996.
21. Berriche, R. Vickers Hardness from Plastic Energy, Scripta Metallurgica et Materialia 32 (4), 617–620, 1995.
22. Li, X. D.; Bhushan, B. A Review of Nanoindentation Continuous Stiffness Measurement Technique and Its Applications, Materials Characterization 48 (1), 11–36, 2002.
23. Freund, L. B.; Suresh, S. *Thin Film Materials: Stress, Defect Formation and Surface Evolution*; Cambridge University Press: Cambridge, UK, 2003.
24. Ohring, M. *Materials Science of Thin Films, Deposition and Structure*; Academic Press: San Diego, CA, 2002.
25. Nix, W. D. Mechanical-Properties of Thin-Films, Metallurgical Transactions A-Physical Metallurgy and Materials Science 20 (11), 2217–2245, 1989.
26. Jankowski, A. F.; Tsakalakos, T. Effects of Deflection on Bulge Test Measurements of Enhanced Modulus in Multilayered Films, Thin Solid Films 291 243–247, 1996.
27. Small, M. K.; Nix, W. D. Analysis of the Accuracy of the Bulge Test in Determining the Mechanical-Properties of Thin-Films, Journal of Materials Research 7 (6), 1553–1563, 1992.
28. Liechti, K. M.; Shirani, A. Large-Scale Yielding in Blister Specimens, International Journal of Fracture 67 (1), 21–36, 1994.
29. Petersen, K. E.; Guarnieri, C. R. Youngs Modulus Measurements of Thin-Films Using Micromechanics, Journal of Applied Physics 50 (11), 6761–6766, 1979.
30. Osterberg, P. M.; Senturia, S. D. M-TEST: A Test Chip for MEMS Material Property Measurement Using Electrostatically Actuated Test Structures, Journal of Microelectromechanical Systems 6 (2), 107–118, 1997.
31. Weihs, T. P.; Hong, S.; Bravman, J. C.; Nix, W. D. Mechanical Deflection of Cantilever Microbeams – A New Technique for Testing the Mechanical-Properties of Thin-Films, Journal of Materials Research 3 (5), 931–942, 1988.
32. Dauskardt, R.; Lane, M.; Ma, Q.; Krishna, N. Adhesion and Debonding of Multi-Layer Thin Film Structures, Engineering Fracture Mechanics 61 (1), 141–162, 1998.
33. Volinsky, A. A.; Moody, N. R.; Gerberich, W. W. Interfacial Toughness Measurements for Thin Films on Substrates, Acta Materialia 50 (3), 441–466, 2002.
34. Lane, M. Interface Fracture, Annual Review of Materials Research 33 29–54, 2003.
35. Thouless, M. D. Cracking and Delamination of Coatings, Journal of Vacuum Science and Technology A-Vacuum Surfaces and Films 9 (4), 2510–2515, 1991.
36. Hutchinson, J. W.; Suo, Z. Mixed-Mode Cracking in Layered Materials, Advances in Applied Mechanics, 29, 63–191, 1992.
37. Beuth, J. L. Cracking of Thin Bonded Films in Residual Tension, International Journal of Solids and Structures 29 (13), 1657–1675, 1992.
38. Marshall, D. B.; Evans, A. G. Measurement of Adherence of Residually Stressed Thin-Films by Indentation .1. Mechanics of Interface Delamination, Journal of Applied Physics 56 (10), 2632–2638, 1984.

39. Kriese, M. D.; Gerberich, W. W.; Moody, N. R. Quantitative Adhesion Measures of Multilayer Films: Part I. Indentation Mechanics, Journal of Materials Research 14 (7), 3007–3018, 1999.
40. Kriese, M. D.; Gerberich, W. W.; Moody, N. R. Quantitative Adhesion Measures of Multilayer Films: Part II. Indentation of W/Cu, W/W, Cr/W, Journal of Materials Research 14 (7), 3019–3026, 1999.
41. Volinsky, A. A.; Moody, N. R.; Gerberich, W. W. Interfacial Toughness Measurements for Thin Films on Substrates, Acta Materialia 50 (3), 441–466, 2002.
42. Charalambides, M. Fracture Mechanics Specimen for Interface Toughness Measurement, Journal of Applied Mechanics 56 (0), 77–82, 1989.
43. Hofinger, I.; Oechsner, M.; Bahr, H. A.; Swain, M. V. Modified Four-Point Bending Specimen for Determining the Interface Fracture Energy for Thin, Brittle Layers, International Journal of Fracture 92 (3), 213–220, 1998.
44. Becker, T. L.; McNaney, J. M.; Cannon, R. M.; Ritchie, R. O. Limitations on the Use of the Mixed-Mode Delaminating Beam Test Specimen: Effects of the Size of the Region of K-Dominance, Mechanics of Materials 25 (4), 291–308, 1997.
45. Mönig, R.; Keller, R. R.; Volkert, C. A. Thermal Fatigue Testing of Thin Metal Films, Review of Scientific Instruments 75 (11), 4997–5004, 2004.
46. Keller, R. R.; Geiss, R. H.; Cheng, Y.-W.; Read, D. T. IMECE2004-61291: Microstructure Evolution During Alternating-Current-Induced Fatigue, in Proceedings of the International Mechanical Engineering Conference and Exposition 2004; American Society of Mechanical Engineers: 2004; pp. 107–112.
47. Geiss, R. H.; Read, D. T.; Keller, R. R. TEM Study of Dislocation Loops in Deformed Aluminium Films, Microscopy and Microanalysis 11 (S02), 1870–1871, 2005.
48. Keller, R. R.; Geiss, R. H.; Barbosa, N.; Slifka, A. J.; Read, D. T. Strain-Induced Grain Growth During Rapid Thermal Cycling of Aluminum Interconnects, Metallurgical and Materials Transactions A-Physical Metallurgy and Materials Science 38A (13), 2263–2272, 2007.
49. Barbosa, N.; Keller, R. R.; Read, D. T.; Geiss, R. H.; Vinci, R. P. Comparison of Electrical and Microtensile Evaluations of Mechanical Properties of an Aluminum Film, Metallurgical and Materials Transactions A-Physical Metallurgy and Materials Science 38A (13), 2160–2167, 2007.

FROM MACRO TO MESO AI
QUANTIZED COHESIVE MC

MICHAEL P. WNU
Department of Civil
Engineering and Ap
Milwaukee, 3200 N.

Abstract A discretization proc
crack requires that all pertinent
cohesive stress that restrains ope
intensity factor, the modulus of
opening displacement within the
are re-visited and replaced by cer
to as either "unit step growth"
aspects of the model enter the th
roughness of the newly created s
pagating crack. Both variables ar
of the cohesive zone. At the poin
the characteristic material length

Novel properties of the prese
effective tool to explain multis
associated transitions from nano
response to deformation and fract
material appear to be inherent defi

As the degree of fractality inc
shown to rapidly grow to the leve
than those predicted for the classi
an unusual size-sensitivity of frac
bonding such as concrete and cert
are commonly observed.

In the limit of vanishing qua
fractality the quantized cohesive r
reduces to the well-known classic
LEFM or the QFM fracture theori

* E-mail: mpw@uwm.edu

G. Pluvinage and A. Sedmak (eds.), *Security a*
and Defective Materials,